about 7000 data points. Of these, 596 data points for optimum angle, 118 data points for optimum thickness, and 271 data points for optimum emissivity are chosen, for which the Q_{im} is a maximum. Correlations are developed for these optimum parameters as

$$\theta_{\mathrm{opt}} = 1.398 R_0^{-0.009} H^{0.251} t^{-0.052} \varepsilon^{0.056}$$

$$t_{\mathrm{opt}} = 0.008 R_0^{0.004} H^{0.627} \theta^{-0.439} \varepsilon^{0.629}$$

$$\varepsilon_{\mathrm{opt}} = 0.869 R_0^{0.006} H^{-0.437} t^{0.264} \theta^{0.706}$$

The correlation coefficients are 0.9916, 0.9937, and 0.9916, respectively. The corresponding maximum errors are 5.7, 9.3, and 9.4%, respectively. Using 1378 data points, a correlation is developed for maximum improvement in heat loss per unit mass:

$$Q_{\mathrm{im,max}} = 0.144 R_0^{0.058} H^{-0.409} t^{-0.796} \theta^{0.291} \varepsilon^{0.444}$$

with a correlation coefficient of 0.9947 and a maximum error of 14.92%. The parameters and range for the correlations are $10 \leq \theta \leq 90$ deg, $0.01 \leq R_0 \leq 0.1$ m, $0.05 \leq H \leq 0.5$ m, $0.2 \leq t \leq 4$ mm, $0.05 \leq \varepsilon \leq 0.95$, $T_B = 313.15$ K, $T_e = 4$ K, $k = 177$ W/m K, and $\rho = 2770$ kg/m^3.

Conclusions

A hollow conical configuration is proposed for space radiator applications, which gives an improvement in heat loss per unit mass of about 4.8 times greater than that of the corresponding solid pin fin. It is found that there exists an optimum angle, thickness, and emissivity for which improvement in heat loss per unit mass is a maximum. The optimum angle increases with increase in height and emissivity and decreases with increase in thickness. The optimum thickness increases with increase in height and emissivity and decreases with increase in angle. The optimum emissivity increases with increase in angle and thickness and decreases with increase in height. Correlations are presented for optimum angle, thickness, emissivity, and corresponding maximum improvement in heat loss per unit mass.

References

[1] Chung, B. T. F., and Zhang, B. X., "Optimization of Radiating Fin Array Including Mutual Irradiations Between Radiator Elements," *Journal of Heat Transfer*, Vol. 113, No. 4, 1991, pp. 814–822.

[2] Sunil Kumar, S., Venketesh, N., and Venkateshan, S. P., "Optimum Finned Space Radiators," *International Journal of Heat and Fluid Flow*, Vol. 14, No. 2, 1992, pp. 191–200.

[3] Sunil Kumar, S., and Venkateshan, S. P., "Optimized Tubular Radiator with Annular Fins on a Non-Isothermal Base," *International Journal of Heat and Fluid Flow*, Vol. 15, No. 5, 1994, pp. 399–409.

[4] Krishnaprakas, C. K., "Optimum Design of Radiating Rectangular Plate Fin Array Extending from a Plane Wall," *Journal of Heat Transfer*, Vol. 118, No. 2, 1996, pp. 490–493.

[5] Krishnaprakas, C. K., "Optimum Design of Radiating Longitudinal Fin Array Extending from a Cylindrical Surface," *Journal of Heat Transfer*, Vol. 119, No. 4, 1997, pp. 857–860.

[6] Krikkis, R. N., and Panagiotis, R., "Optimum Design of Spacecraft Radiators with Longitudinal Rectangular and Triangular Fins," *Journal of Heat Transfer*, Vol. 124, No. 5, 2002, pp. 805–811.

[7] Bhise, Navin V., Katte, Subrahmanya S., and Venkateshan, S. P., "A Numerical Study of Corrugated Structure for Space Radiators," *5th ISHMT-ASME Heat and Mass Transfer Conference*, edited by S. S. Saha, S. P. Venkateshan, B. V. S. S. S. Prasad, and S. S. Sadhal, Tata McGraw–Hill, New Delhi, 2002, pp. 520–526.

[8] Srinivasan, K., and Katte, Subrahmanya S., "Analysis of Grooved Space Radiator," *6th ISHMT-ASME Heat and Mass Transfer Conference*, 2004 (to be published).

[9] Howell, J. R., *Catalog of Radiation Heat Transfer Configuration Factors* [online], URL: http://www.me.utexas.edu/~howell/index.html [cited 15 July 2003].

[10] Kern, D. Q., and Kraus, A. D., *Extended Surface Heat Transfer*, McGraw–Hill, New York, 1972, pp. 204–207.

Radiation with Mixed Convection in an Absorbing, Emitting, and Anisotropic Scattering Medium

Tzer-Ming Chen*
National Taipei University of Technology, Taipei 10643, Taiwan, Republic of China

Nomenclature

f	=	dimensionless stream function
g	=	acceleration of gravity
h	=	heat-transfer coefficient
I	=	dimensionless radiation intensity
k	=	thermal conductivity
N	=	conduction-radiation parameter
Nu_x	=	local Nusselt number
$P_n(\mu)$	=	Legendre polynomial of the first kind of degree n
Pr	=	Prandtl number
$p(\mu, \mu')$	=	phase function
Q^r	=	dimensionless radiative heat flux
q^r	=	radiative heat flux
Re_x	=	local Reynolds number
T	=	temperature
x, y	=	physical coordinates along and normal to the wall
β	=	volumetric coefficient of thermal expansion
β_0	=	extinction coefficient
ε	=	emissivity of plate surface
η	=	nonsimilarity variable
θ	=	dimensionless temperature
λ	=	coefficient of the thermal expansion
μ	=	direction cosine
ν	=	kinematic viscosity
ξ	=	nonsimilarity variable
ρ	=	fluid density
ρ_d	=	diffuse reflectivity of plate surface
$\bar{\sigma}$	=	Stefan–Boltzmann constant
τ	=	optical variable, $= \xi\eta$
φ	=	stream function
Ω	=	buoyancy parameter
ω	=	scattering albedo

Subscripts

w	=	wall
∞	=	external flow

Introduction

THE problem of radiation on mixed convection along a vertical plate with uniform surface temperature has been studied theoretically because the radiation effects on the mixed convection flow are important in the context of space and processes involving high temperature. At high temperatures, thermal radiation can significantly affect the heat transfer and temperature distribution in boundary-layer flow of a participating fluid. Cess,[1] Arpaci,[2] Soundalgekar and Takhar,[3] and Hossain and Takhar[4] have utilized the optically thin limit and the optically thick limit approximation methods for these studies. But these approximations are accurate

Received 29 October 2003; revision received 17 November 2003; accepted for publication 18 November 2003.

*Associate Professor, Department of Vehicle Engineering, No. 1, Sec. 3, Chung-Hsiao East Road.

only within particular optical thickness limits and, therefore, are restricted in applicability. For the complete analysis, Cheng and Ozisik[5] used the normal-mode expansion technique for an absorbing, emitting, and isotropically scattering fluid. To consider the anisotropic scattering effects were studied in the wedge flow by Yucel and Bayazitoglu,[6] Wu et al.,[7] and Chen.[8]

The objective of this investigation is to demonstrate the influences of anisotropic scattering on the mixed convection from a vertical plate with diffuse reflecting surface, and the linear and Rayleigh anisotropic scattering models are employed.

Analysis

Consider a heated, vertical plate at a uniform temperature T_w submerged in an absorbing, emitting, anisotropically scattering, incompressible, gray medium. Figure 1 illustrates the physical geometry. The external flow consists of a uniform freestream with velocity u_∞ and temperature $T_\infty (T_w > T_\infty)$. Under the usual Boussinesq approximation the flow is governed by the following boundary-layer equations:

$$\frac{\partial u}{\partial x} + \frac{\partial v}{\partial y} = 0 \tag{1a}$$

$$u\frac{\partial u}{\partial x} + v\frac{\partial u}{\partial y} = \nu\frac{\partial^2 u}{\partial y^2} + g\lambda(T - T_\infty) \tag{1b}$$

$$u\frac{\partial T}{\partial x} + v\frac{\partial T}{\partial y} = \frac{k}{\rho c_p}\frac{\partial^2 T}{\partial y^2} - \frac{1}{\rho c_p}\frac{\partial q^r}{\partial y} \tag{1c}$$

with the boundary conditions

$$u = v = 0, \qquad T = T_w \quad \text{at} \quad y = 0 \tag{2a}$$

$$u = u_\infty, \qquad T = T_\infty \quad \text{at} \quad y \to \infty \tag{2b}$$

The continuity is satisfied by the introduction of a stream function φ, and we introduce the following transformations to recast the boundary-layer equations:

$$\theta = \frac{T}{T_\infty}, \qquad \theta_w = \frac{T_w}{T_\infty} \tag{3a}$$

$$N = \frac{k\beta_0}{4n^2\bar{\sigma}T_\infty^3}, \qquad Q^r = \frac{q^r}{4n^2\bar{\sigma}T_\infty^4} \tag{3b}$$

$$f(x,\eta) = (\nu u_\infty x)^{-(\frac{1}{2})}\varphi(x,y) \tag{3c}$$

$$\eta = y\left(\frac{u_\infty}{\nu x}\right)^{\frac{1}{2}}, \qquad \xi = \beta_0 x Re_x^{-(\frac{1}{2})} \tag{3d}$$

$$\Omega = \frac{g\beta T_\infty}{\beta_0^2 \nu u_\infty}, \qquad Pr = \frac{\rho c_p \nu}{k} \tag{3e}$$

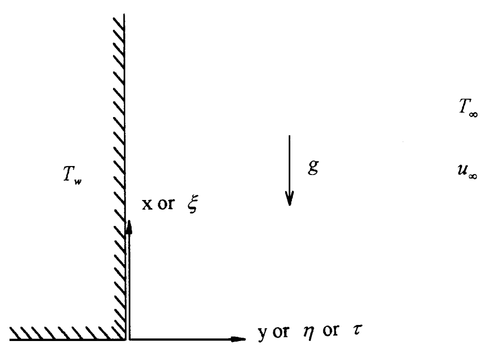

Fig. 1 Geometry and coordinate system of the physical model.

These transformations reduce Eq. (1) to

$$f''' + \frac{1}{2}ff'' + \Omega(\theta - 1)\xi^2 = \frac{1}{2}\xi\left(f'\frac{\partial f'}{\partial \xi} - f''\frac{\partial f}{\partial \xi}\right) \tag{4a}$$

$$\frac{1}{Pr}\theta'' + \frac{1}{2}f\theta' = \frac{1}{2}\xi\left(f'\frac{\partial \theta}{\partial \xi} - \frac{\partial f}{\partial \xi}\theta'\right) + \frac{\xi}{NPr}Q^{r'} \tag{4b}$$

The boundary conditions (2) become

$$f = f' = 0 \quad \text{and} \quad \theta = \theta_w \quad \text{at} \quad \eta = 0 \tag{5a}$$

$$f' = 1 \quad \text{and} \quad \theta = 1 \quad \text{at} \quad \eta \to \infty \tag{5b}$$

The radiation part of this problem satisfies the equation of radiative transfer given in the form

$$\mu\frac{\partial I}{\partial \tau} + I = (1 - \omega)\frac{\theta^4}{4\pi} + \frac{\omega}{2}\int_{-1}^{1} p(\mu,\mu')I(\tau,\mu')\,\mathrm{d}\mu' \tag{6a}$$

where

$$p(\mu,\mu') = \sum_{n=0}^{N} a_n P_n(\mu)P_n(\mu'), \qquad a_0 = 1 \tag{6b}$$

and the boundary conditions

$$\tau = 0, \qquad I^+(0,\mu) = \frac{\varepsilon\theta_w^4}{4\pi} + 2\rho_d\int_0^1 I^-(0,-\mu')\mu'\,\mathrm{d}\mu' \qquad \mu > 0 \tag{7a}$$

$$\tau \to \infty, \qquad I^-(\tau,-\mu) = \frac{1}{4\pi}, \qquad \mu > 0 \tag{7b}$$

The net heat flux at the wall in term of the dimensionless quantities is expressed as

$$Q_w = \frac{q_w}{4n^2\bar{\sigma}T_\infty^4} = \left(-N\frac{\partial \theta}{\partial \tau} + Q^r\right)_{\tau=0} = \left(-\frac{N}{\xi}\frac{\partial \theta}{\partial \eta} + Q^r\right)_{\eta=0} \tag{8}$$

The local Nusselt number for the combined mixed convection and radiation becomes

$$Nu_x Re_x^{-(\frac{1}{2})} = [1/(\theta_w - 1)][-\theta' + (\xi/N)Q^r]_{\eta=0} \tag{9}$$

Results and Discussion

The Galerkin method[9] and the Keller box method[10] have been used to analyze the problem of simultaneous mixed convection and radiation from a vertical plate for an absorbing, emitting, and anisotropic scattering medium.

The influences of the scattering albedo ω and the forward-backward-scattering parameters a_1 on the value of the local Nusselt number are represented in Fig. 2. The effect of the scattering albedo

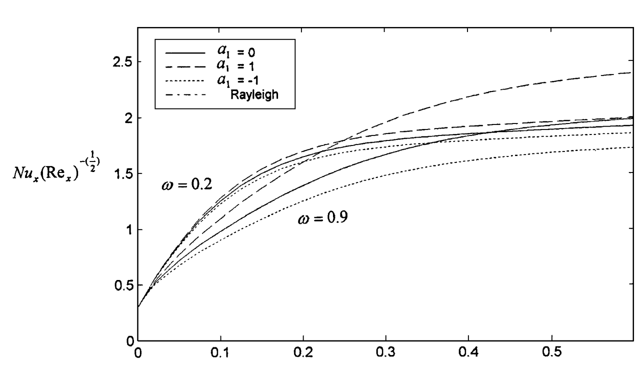

Fig. 2 Effects of the scattering albedo ω on the value of the Nusselt number for $Pr = 0.733$, $N = 0.1$, $\rho_d = 0$, $\Omega = 1$, and $\theta_w = 1.2$.

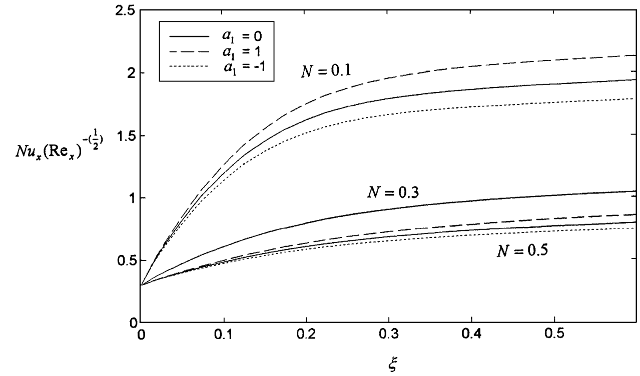

Fig. 3 Effects of the conduction-radiation parameter N on the value of the local Nusselt number for $Pr = 0.733$, $\omega = 0.5$, $\rho_d = 0$, $\Omega = 1$, and $\theta_w = 1.2$.

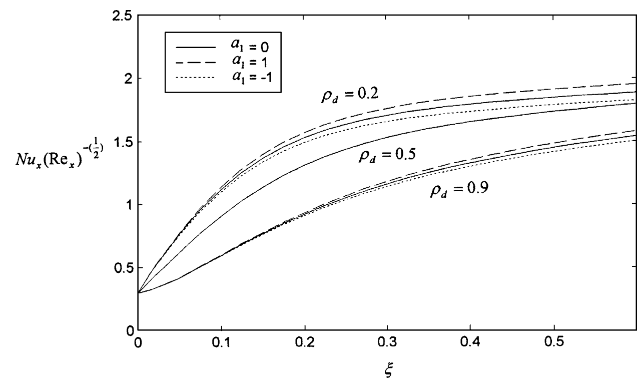

Fig. 4 Effects of the surface reflectivity ρ_d on the value of the local Nusselt number for $Pr = 0.733$, $\omega = 0.2$, $N = 0.1$, $\Omega = 1$, and $\theta_w = 1.2$.

is to decrease the value of the total heat flux at small values of ξ but to increase at large values of ξ, and the forward-backward-scattering parameter a_1 has a significant effect on the heat transfer. The value of the local Nusselt number for a strong backward-scattering fluid ($a_1 = -1$) with $\omega = 0.2$ is about 2.0% less than that for a strong forward-scattering fluid ($a_1 = 1$) at $\xi = 0.1$ and 3.5% less at $\xi = 0.6$, and the respective percentages are 21 and 38% for $\omega = 0.9$. The anisotropic scattering effects on the value of the local Nusselt number are amplified at large values of ω and the difference between the isotropic and Rayleigh scattering is small.

Figure 3 represents the variation of the local Nusselt number with the conduction-radiation parameter N, which characterizes the relative importance of radiation in regard to conduction. It is observed that the value of the local Nusselt number increases as the value of N decreases and the anisotropic scattering effects on the heat flux are amplified at small values of N.

Figure 4 shows the influence of the surface reflectivity. It is found that the value of the local Nusselt number decreases with the increase of surface reflectivity ρ_d. This is because the reflection at the surface increases the path length of radiative transfer.

Conclusions

From this study, the following is found:

1) The influence of the optical thickness τ_∞ is that the value of the net radiative heat flux and the local Nusselt number decreases as the optical thickness τ_∞ increases.

2) The effect of the scattering albedo ω is to decrease the value of the local Nusselt number at small values of ξ but to increase at large values of ξ.

3) The forward-backward-scattering parameter a_1 has a significant effect on the heat transfer.

4) The increase in the value of the local Nusselt number reduces the value of the conduction-radiation parameter N.

5) The value of local Nusselt number decreases with the increase of the value of surface reflectivity ρ_d.

6) The value of the local Nusselt number increases as the wall temperature increases.

References

[1]Cess, R. D., "The Interaction of Thermal Radiation with Free Convection Heat Transfer," *International Journal of Heat Mass Transfer*, Vol. 9, 1966, pp. 1269–1277.

[2]Arpaci, V. S., "Effect of Thermal Radiation on the Laminar Free Convection from a Heated Vertical Plate," *International Journal of Heat Mass Transfer*, Vol. 11, 1968, pp. 871–881.

[3]Soundalgekar, V. M., and Takhar, H. S., "Radiative Free Convection Flow of a Gas past a Semi-Infinite Vertical Plate," *Journal of Modern Measuring Contraction*, Vol. B51, 1993, pp. 31–40.

[4]Hossain, M. A., and Takhar, H. S., "Radiation Effect on Mixed Convection along a Vertical Plate with Uniform Surface Temperature," *International Journal of Heat and Mass Transfer*, Vol. 31, 1996, pp. 243–248.

[5]Cheng, E. H., and Özisik, M. N., "Radiation with Free Convection in an Absorbing, Emitting and Scattering Medium," *International Journal of Heat and Mass Transfer*, Vol. 15, 1972, pp. 1243–1252.

[6]Yücel, A., and Bayazitoglu, Y., "Radiative Heat Transfer in Absorbing, Emitting, and Anisotropically Scattering Boundary-Layer Flows," *AIAA Journal*, Vol. 22, No. 8, 1984, pp. 1162–1166.

[7]Wu, C. Y., Wu, S. C., and Chen, C. K., "Radiative Heat Transfer in Anisotropically Scattering Boundary-Layer Flows in Diffusely Reflecting Boundaries," *Proceedings of the Sixth International Numerical Methods in Thermal Problems Conference*, Vol. 6, Pt. 1, 1989, pp. 773–782.

[8]Chen, T. M., "Radiative Heat Transfer in Anisotropically Scattering Boundary-Layer Flows with Reflecting Boundaries," *International Journal of Heat and Mass Transfer*, Vol. 32, 1997, pp. 411–417.

[9]Cengel, Y. A., and Özisik, M. N., "The Use of the Galerkin Method for Radiation Transfer in an Anisotropically Scattering Slab with Reflecting Boundaries," *Journal of Quantum Spectroscopy Radiative Transfer*, Vol. 32, No. 3, 1984, pp. 225–233.

[10]Cebeci, T., and Bradshaw, P., *Momentum Transfer in Boundary Layers*, Hemisphere, Washington, DC, 1977.

Coupled Radiation and Conduction in a Graded Index Layer with Specular Surfaces

Yong Huang,* Xin-Lin Xia,† and He-Ping Tan‡

Harbin Institute of Technology, 150001 Harbin, People's Republic of China

Nomenclature

a_i	=	coefficient denoting temperature effect of node i on $I(x_k, \zeta_p)$
B_{ik}	=	coefficient denoting radiative effect of node i on thermal balance of node k
B'_{ik}	=	coefficient denoting temperature effect of node i on radiative flux of node k
d	=	thickness of medium layer, m
h	=	convective heat transfer coefficient, W/m$^2 \cdot$ K
$I^*(j)$	=	radiative intensity at the jth tracing point, W/m$^2 \cdot$ sr

Received 27 August 2002; revision received 7 October 2003; accepted for publication 2 November 2003.

*Ph.D. Candidate, School of Energy Science and Engineering, 92 West Dazhi Street; huangly_zl@263.net.

†Professor, School of Energy Science and Engineering, 92 West Dazhi Street; xiaxl@hit.edu.cn.

‡Professor, School of Energy Science and Engineering, 92 West Dazhi Street.